Magnetic orientational phase transition in a real crystal

V. K. Vlasko-Vlasov, L. M. Dedukh, M. V. Indenbom, and V. I. Nikitenko

Institute of Solid State Physics, USSR Academy of Sciences

A direct study is made of orientational phase transitions in dislocation-containing single crystals of gadolinium iron garnet in a magnetic field applied along the $\langle 111 \rangle$ easy axis. The observed shape of the boundary of the collinear and canted phases in the stress field of an individual dislocation agrees well with the theoretically calculated one. The change of the $H - T$ phase diagram of orientational first-order phase transitions is investigated as a function of the distance to the dislocation. The experimentally constructed phase diagrams for different points of the crystal are well described by the theoretical curves calculated with account taken of the induced anisotropy. Certain microscopic parameters of gadolinium iron garnets are obtained on the basis of the obtained experimental dependences.

PACS numbers: 75.30.Kz, 75.50.Gg, 61.70.Jc

It has by now become obvious that the construction of phase-transition theory that describes with quantitative rigor the experimental data is impossible without allowance for the real structure of the crystals. The theoreticians therefore resort more and more frequently to an elucidation of the role of the pointlike, linear, and other defects of the crystal lattice in the formation of the processes that determine the phase transitions.[1-4] Exceedingly useful for the development of this theory may be experimental research into spin-flip transitions, due to the change of direction of the spontaneous magnetization vectors of the magnetic sublattices of the crystal with changing temperature T or with changing external magnetic field H in transparent magnetic dielectrics.[5] For an experimental study of these phase transitions one can use not only traditional methods of measuring the macroscopic properties of the material, but also polarization-optical methods of local analysis of the state of the magnetic and real structures of the sample, thereby uncovering possibilities of studying their interaction in the course of the transition.

The first magneto-optical investigations have shown that in strong magnetic fields, when magnetization in ordinary ferromagnets is due only to the paraprocess, the magnetic structure of multisublattice crystals changes and domains of different phases are formed. Observation of the transformation of the domain structure as a function of T and H has made it possible to construct diagrams of spin-flip transitions.[6,7]

The main laws that govern magnetic orientational transitions were described with account taken of the exchange interaction between the magnetic sublattices and the magnetocrystalline anisotropy.[5] Up to now, however, no full agreement was obtained between the predictions of the theory and the experimental data. Thus, on the basis of the model of a multisublattice ferrimagnet with ideal cubic anisotropy, it is impossible to explain the coexistence of various phases in an unexpectedly large temperature interval,[6] a number of observed regularities of the transition between the canted phases,[7] and the substantial difference between the characteristics of the phase diagrams obtained by different authors

that have used the same iron garnets (e.g., the data for the gadolinium iron garnet[6-14]). Such disparities between theory and experiment are attributed to the inhomogeneities of the composition and to internal stresses in the crystals,[5] but up to now no consistent investigation has been made of the influence of any elementary sources of internal stresses on the orientational phase transitions. This has greatly hindered the development of a theory for these phenomena.

Observation of singularities in the course of the spin-flip phase transition near an individual dislocation in single-crystal gadolinium iron garnets was first reported in Ref. 15. In the present study we have investigated experimentally and theoretically the diagram of the orientational phase transition in single-crystal gadolinium iron garnets, with allowance for the stresses produced by single dislocations. We show that the magnetic anisotropy induced by the inhomogeneous internal stresses influences substantially both the form of the diagram of the phase transition and its kinetics.

EXPERIMENTAL PROCEDURE

The samples used in the experiment were cut from a single-crystal gadolinium iron garnet $(Gd_3Fe_5O_{12})$ grown from the solution in a melt, parallel to the $(1\bar{1}0)$ plane, and the subjected to mechanical and chemical polishing. The obtained plates, 30–40 μm thick, were placed in a cryostat between a copper washer and a cold finger through which heated liquid-nitrogen vapor was passed. The temperature was measured with a copper-constantan thermocouple accurate to $\pm$ 0.02 K. The cryostat was placed between the poles of an electromagnet that produced a constant field of intensity up to 22 kOe, measured with a Hall pickup and applied along the easy magnetization axis $[11\bar{1}]$ that lies in the plane of the sample. The direction of this easy-magnetization axis was revealed, at temperatures far from the compensation point, by the 180-deg boundary that separated two Cotton domains and was practically perpendicular to the $(1\bar{1}0)$ plane of the sample. At these temperatures, the magnetization of the gadolinium iron garnet is high enough to make this

boundary flat and parallel to the magnetization vectors of the domains that lie along the easy axis [11$\bar{1}$]. The orientation of the dislocation glide plane was determined from the birefringence rosette[16] observed around the dislocation in crossed polarizers, when the sample was magnetized tangentially to its surface. The identification of thre magnetic phases was based on a determination of the directions of the sublattice magnetization vectors with the aid of the Faraday and the Cotton-Mouton effects in polarized light.

All the investigated samples had an inhomogeneous structure, and the first-order phase transitions between the collinear and canted phases[5] took place in them predominantly via nucleation of new phases and gradual displacement of their interphase boundaries. The temperature at which the investigated interphase boundary passed through a fixed point of the sample was assumed (without allowance for the influence of the surface tension of this boundary) equal to the equilibrium temperature of the phase transition at this point. The dependence of the transition temperature on the external magnetic field at various points of the crystal determined the line of the phase transitions on the $H - T$ plane. It was most convenient to plot each such line in the experiment by returning the investigated interphase boundary to the chosen point via a change in the field H while the temperature in the cryostat was slowly decreased or increased.

EXPERIMENTAL RESULTS

In the investigated $Gd_3Fe_5O_{12}$ samples, in accord with the theory,[5] in a magnetic field parallel to the [11$\bar{1}$] easy axis, we observed four phases: two collinear (the magnetization of the gadolinium sublattice was directed along the field in the low-temperature phase and against the field in the high-temperature field), and two canted. However, out of the three possible planes of rotation of the magnetic moment of the canted phases[5] for an ideal crystal with cubic magnetic anisotropy, only one was realized. The high-temperature and low-temperature canted phases could be easily distinguished visually, using slightly uncrossed Nicol prisms, by the difference in brightness and coloring. The collinear phases could be distinguished by observing the motion of their boundaries with the canted phases as the magnetic field and temperature were varied.

A transition between the collinear phases and the corresponding canted phases, via gradual displacement of an interphase boundary through the entire sample in a constant magnetic field $H \lesssim 0.5$ kOe, took place when the temperature was changed by several degrees. With increasing external field, the temperature interval of the transition decreased to approximately 0.5 K and remained practically constant at $H \gtrsim 3$ kOe. It was determined to a great degree by the crystal-lattice defects which influenced both the nucleation of the new phase and the character of the interphase-boundary motion. The magnetic orientational transition in a constant field H||[11$\bar{1}$] equal to 177 Oe, near a single 60-deg dislocation with a glide plane (11$\bar{1}$) and axis [1$\bar{1}$0], is illustrated in Fig. 1. When the temperature approached from below the compensation point T_c, equal to 282.5 K in the vicinity of the dislocation, a low-temperature canted phase D, in the

form of a light three-lobe rosette, appeared against the background of the collinear phase B, in which the magnetization M||[11$\bar{1}$] was in the plane of the plate (Fig. 1a). One of the lobes of the rosette was considerably smaller than the other two. The region occupied by the phase D in Fig. 1 is brighter than its surrounding dark region of the phase B, since the magnetization of the iron sublattices in the phase D emerged from the plane of the sample, causing Faraday rotation of the plane of polarization of the light.

With increasing temperature, the rosette of the canted phase on the dislocation increased and emerged with the macroscopic region of the same phase advancing from the volume of the sample (Fig. 1b). In the course of the subsequent successive (Fig. 1c) redistribution of the volume fractions of the phases B and D, their sectorial arrangement in definite sections of the dislocation field of the microstresses was rigorously preserved. The collinear phase B, decreasing, formed a rosette (Fig. 1d) symmetric, relative to the dislocation axis, to the phase-D rosette that existed at lower temperatures (Fig. 1a). The phase B vanished at 284 K.

A similar process took place when the temperature approached T_c from above. The picture of the replacement of the high-temperature collinear phase A by the high-temperature canted phase C is practically identical to that considered above, apart from the replacement of the corresponding values of T (see Fig. 1) by $2T_c - T$. The magnetization of the iron sublattices in the region of the high-temperature phase C, just as in the D phase, was along the [11$\bar{1}$] axis, and the form of the magnetic rosettes produced on the dislocation was the same as in Fig. 1 for the low-temperature transition.

Within the volume of the sample, the low-temperature and high-temperature transitions proceeded in similar fashion: In both temperature intervals that are symmetrical about T_c, the moving interphase boundaries were similar in shape in the transitions $B \leftrightarrow D$ and $C \leftrightarrow A$.

The transition between the high- and low-temperature phases of the same type (both between collinear and between canted phases) was due to the motion, through the crystal, of an interphase boundary identical in character with a 180-deg compensation boundary.[17] In magnetic fields $H \gtrsim 0.5$ kOe at $T \approx 283$ K, the incipient new phase was bounded by such a compensation boundary that moved through the entire crystal with further decrease of temperature (by approximately 0.5 K). In weaker fields $H \lesssim 0.5$ kOe, the transition between the high- and low-temperature phases took place at $T \approx 282.5$ K so rapidly that it was impossible to follow the displacements of the interphase boundaries.

The character of the influence of the defects of the crystal lattice on the compensation boundary differed substantially from their influence on the boundary between the collinear and canted phases. The phases of the 180-deg neighborhood, separated by such a boundary, were equivalent with respect to the internal stresses. Therefore the direction of the approach of the compensation boundary to the dislocation was determined by factors that were not connected with the dislocation stress field. Accordingly, the equivalent phases in the process of the transition did not form characteristic rosettes on the dislocation. The compensation
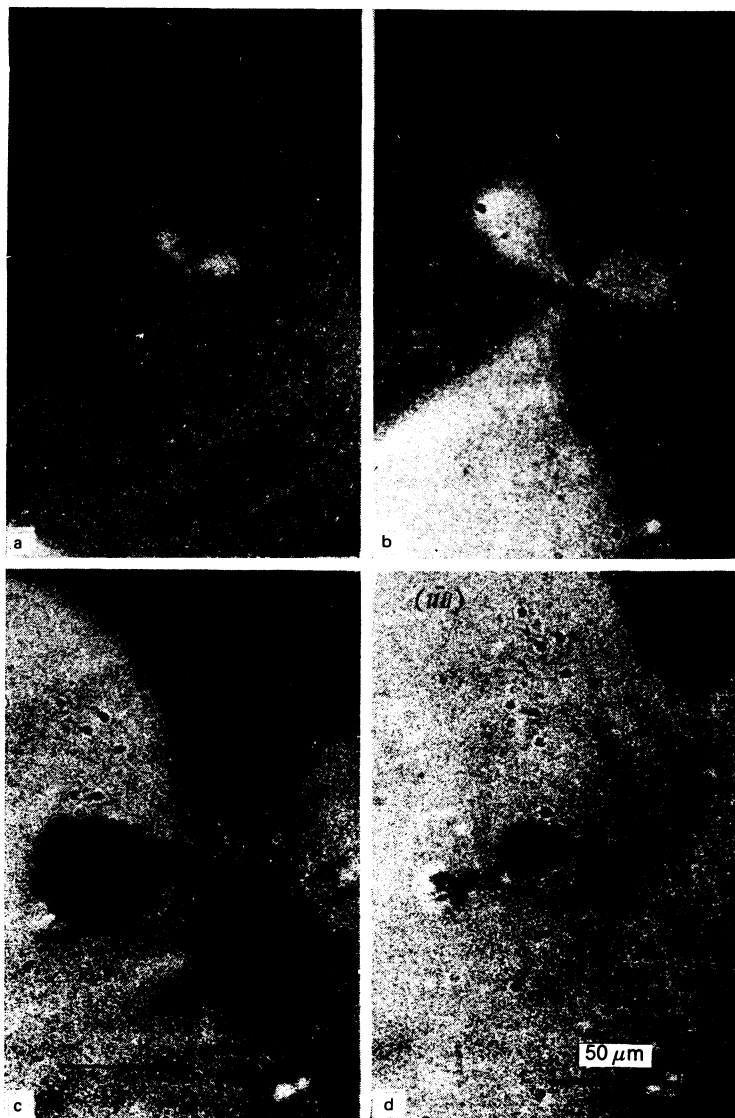
FIG. 1. Change of the shape of the interphase boundary near a dislocation in the course of a spin-flip transition in an external magnetic field H∥[11$\bar{1}$] (the Nicol prisms are slightly uncrossed): a) $T = 280.6$ K; b) $T = 281.0$ K; c) $T = 281.7$ K; d) $T = 282.1$ K; $H = 177$ Oe.

boundary was only pinned to the dislocation and broadened to form two dark lobes corresponding to the collinear phase (Fig. 2). Thus, the dislocation stresses produced from the 180-deg boundary a collinear phase whose region of existence broadened somewhat.

With increasing field, besides the shortening of the region occupied by the collinear phase (the dark region on the top of Fig. 2), the broadening of the boundary near the dislocation decreased and at $H \gtrsim 2$ kOe was already practically unresolved.

To explain the mechanisms whereby the dislocation influences the phase spin-flip transition around it, we investigated the spatial distribution of the transition temperatures. The angular dependence of the transition temperature is described by the form of the interphase boundary (see Figs. 1a and 1d), and its change with increasing distance from the dislocation core was obtained from measurements of tem-

perature dependence of the size of the magentic-rosette lobe. The change of the temperatures of the first-order low- and high-temperature transitions as functions of the reciprocal distance to the dislocation axis along the [111] direction at $H = 170$ Oe is shown in Fig. 3. The experimental points correspond to temperatures T at which the dimension of the dislocation-rosette lobe directed along [111] assumed the corresponding values R. In this case the collinear-phase lobe (the dark rosettes, Fig. 1) was assigned negative values of R, and canted-phase (light) lobe positive values to take into account their symmetry with respect to the dislocation axis. It can be seen from Fig. 3 that the experimental point fit well straight lines. This indicates a linear connection between the temperature of the spin-flip transition and the dislocation stresses which are inversely proportional to the distance from the dislocation core. All lines have equal slope within the limits of measurement accuracy, $dT/dR^{-1} = 1.54$

FIG. 2. Pinning of a 180-deg compensation interface between the high- and low-temperature canted phases by a dislocation: $T = 282.5$ K; $H = 280$ Oe (the Nicol prisms are crossed). The dislocation axis is marked by an arrow.
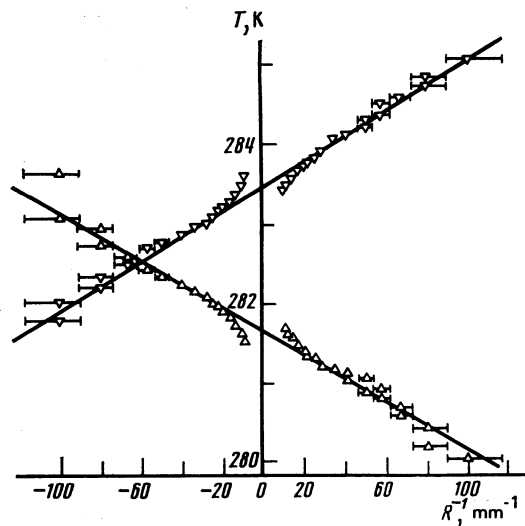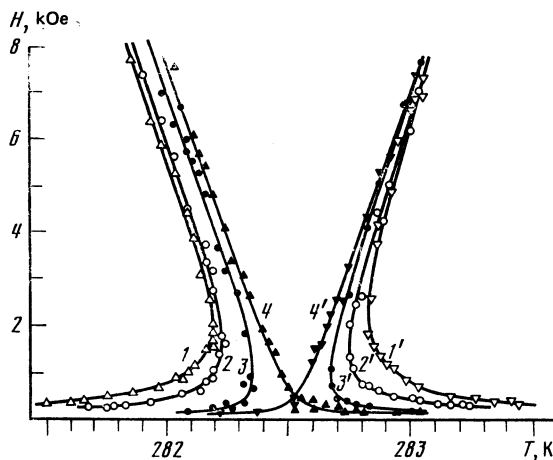

FIG. 4. Local phase diagrams in the vicinity of the dislocation at a distance R from its axis in the [111] direction. 1, 1') $R = 13$ μm; 2, 2') $R = 35$ μm; 3, 3') $R = -35$ μm; 4, 4') $R = -13$ μm respectively at low- and high-temperature transitions from the collinear into the canted phase.

FIG. 3. Dependence of the temperature of the transition between the canted and collinear phases on the reciprocal distance R^{-1} from the dislocation core along the [111] direction. $R > 0$ in the growth direction of the canted-phase lobe. $\triangle$ and $\triangledown$—experimental low- and high-temperature phase-transition points; $H = 170$ Oe.

$\times 10^{-3}$ deg cm. A straight line with negative slope corresponds to a low-temperature transition from the collinear to the canted phase, and one with positive slope to a high-temperature transition. The deviation of the experimental points from straight lines at $|R| \gtrsim 100$ μm is due to the influence of other sources of stresses that distort the elastic field of the considered dislocation and lead to a change in the form of the dislocation rosette when its dimensions exceed ~ 100 μm.

In accordance with these data, a distribution was made between the phase diagrams, plotted in coordinates T and H, at different points of the crystal in the vicinity of the dislocation. Figure 4 shows the $H - T$ diagrams of the phase transitions, plotted by the method described above, in four points that are symmetric about the dislocation and are located at different distances from each (each plotted line corresponds to values of T and H at which the size of the lobe of the magnetic dislocation rosette (see Fig. 1) in the [111] direction retained a fixed value of R). It can be seen that in local sections of the crystal situated on one side ($R > 0$) of the dislocation, the $H - T$ diagram does not undergo fundamental changes as the dislocation is approached, whereas from the opposite side ($R < 0$) the diagram changes qualitatively when the distance to the dislocation is decreased. At the point where the transition takes place from a diverging diagram (curves 1–3) to an intersecting one (curve 4), as will be shown later on, the dislocation microstresses and the stresses from other sources cancel each other. Some mismatch of the centers of the phase diagrams at different points near the dislocation is due to the variation of T_c over the sample, due apparently to the inhomogeneity of the sample composition.

There is no phase-transition line between the low- and high-temperature phases in Fig. 4. An investigation of this transition with the aid of stabilization of the position of the compensation boundary in the vicinity of the dislocation is made difficult by the fact that the boundary is easily attracted to the dislocation core (see Fig. 2) and is retained by it in a large temperature interval.

162   Sov. Phys. JETP 57 (1), January 1983
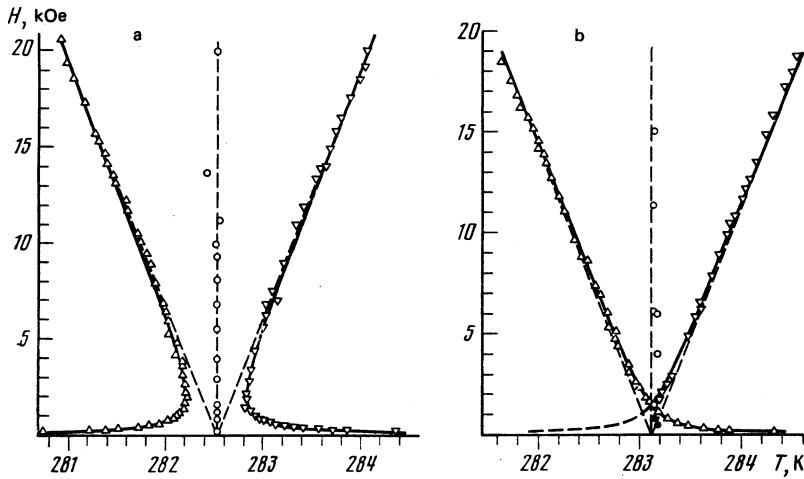
Vlasko-Vlasov et al.   162

FIG. 5. Phase diagrams plotted at crystal points where the induced anisotropy enhances (a) and hinders (b) the formation of the canted phase: $\triangle$—transition between low-temperature collinear and canted phases; $\triangledown$—transition between high-temperature canted and collinear phases; O—transition between canted phases (180-deg rotation of the sublattice magnetization), ●—transition between low- and high-temperature collinear phases.

More correctly plotted were the phase diagrams far from the dislocations, in the crystal section in which the curvature of the interphase boundaries was insignificant and therefore their surface tension influenced the measurement results less. In these regions with low inhomogeneity of the internal stresses, the displacements of the boundaries of the canted and nonlinear phases under the influence of a weak change of temperature were much larger than in the vicinity of the dislocation. This made it possible to determine the phase-transition temperature more accurately. In crystal sections that are far from the dislocations it is easy to fix the instants at which the compensation boundary passes through them when the temperature is changed. The form of the phase diagrams obtained at different points of the crystal depends substantially on whether the induced anisotropy at these points contributes to the appearance of a canted phase, as in the case of curves 1–3 of Fig. 4, or whether it hinders it, as at the point corresponding to curve 4. Both cases are shown in Fig. 5. In Fig. 5b, in the metastable region of existence of high-temperature phases at $T < T_c = 283.1$ K, there is no experimental phase-transition line, inasmuch as in the corresponding magnetic field the temperature of this high-temperature transition is lower than the temperature of nucleation of the compensation boundary in the region with the larger value of T_c.

At $H > 5$ kOe, in all cases, the asymptotes of the experimental points are straight lines (shown dashed in Fig. 5) passing through T_c and having a slope $|dH/dT| \approx 12.8$ kOe/deg. The compensation-boundary motion which causes the transition between the low- and high-temperature phases, took place through the chosen sections of the crystal at different field-independent temperatures $T = T_c$.

PHASE DIAGRAM OF IRON GARNET NEAR THE MAGNETIC-COMPENSATION TEMPERATURE

An analysis, based on the general theory,[5] of the change of the diagram of the considered phase transition under the influence of an induced anisotropy having arbitrary form and due to internal stresses or to other factors, is extremely complicated and has never been carried out. All that was calculated theoretically was the phase diagram for the case of strong uniaxial anisotropy with an axis parallel to the magnetic field applied along the $\langle 111 \rangle$ direction.[18] The spin-flip transition in the experimentally investigated region of relatively weak magnetic fields can be described by a simplified theory that makes it easy to calculate the phase diagram in a real crystal.

We take into account the circumstances that in a weak magnetic field and at an induced magnetic anisotropy lower than cubic, the magnetization vectors of the sublattices of a rare-earth iron garnet deviate insignificantly from an easy-magnetization axis such as $\langle 111 \rangle$, and remain practically collinear. In this case, at sufficient compensation of the sublattice magnetizations, the susceptibility in a field perpendicular to the easy axis, $\chi_\perp$, due to a kink of the sublattices, is larger than the longitudinal susceptibility $\chi_\parallel$ due mainly to the change in the magnetization of the rare-earth sublattices. The canted phase near T_c in an external magnetic field is therefore energetically favored. The magnetocrystalline-energy difference between the phases, which appears at a weak deviation of the magnetization of the sublattices from the corresponding directions of the easy axis $\langle 111 \rangle$, is much less than the energy connected with the susceptibilities $\chi_\parallel$ and $\chi_\perp$. In first-order approximation this contribution of the cubic anisotropy can therefore be neglected, and subsequently its influence affects only the choice of the possible directions of the easy axis.

Neglecting the intrinsic exchange of the rare-earth ions the dependence of the magnetization M_R of their sublattice on the field H and on the temperature T is expressed in terms of the Brillouin function $B_s(x)$ (Ref. 5):

$$M_R = M_R^0 B_s(x), \tag{1}$$

where $x = \mu_R H_{\text{eff}}/kT$, μ_R is the magnetic moment of the

ion, $\mathbf{H}_{eff} = \mathbf{H} + \lambda \mathbf{M}_{Fe}$ is the effective field acting on the rare-earth sublattice $\mathbf{M}_{Fe} = \mathbf{M}_1 + \mathbf{M}_2$ is the total magnetization of the iron sublattices, λ is the effective parameter of the exchange interaction of the rare-earth sublattice with the iron sublattices, k is the Boltzmann's constant, and $M_R^0 = M_R$ at $T = 0$ K. Near the compensation point (where $M_R = -M_{Fe}$ at $H = 0$) the dependence of the resultant magnetization on the temperature can be easily expressed in terms of the longitudinal susceptibility $\chi_\parallel$:

$$M_{Fe} - M_R = [(T - T_c)/T_c] \chi_\parallel \lambda M_{Fe}. \tag{2}$$

Then, taking into account the assumptions made, the energy of the magnetic phase of the iron garnet takes the form

$$E = -\tfrac{1}{2} (\chi_\perp - \chi_\parallel) H^2 \sin^2 \theta - \tfrac{1}{2}\chi_\parallel H^2$$
$$- [(T - T_c)/T_c]\chi_\parallel \lambda M_{Fe} H \cos \theta + \varepsilon, \tag{3}$$

where θ is the angle between the easy axis along which the magnetic moments of the sublattices are oriented and the external field H, while ε is the energy increment due to the elastic stresses or to be the noncubic anisotropy induced in the course of the crystal growth. Under the conditions of our problem $\cos\theta = \pm 1$ for collinear phases and $\cos\theta = \pm 1/3$ for canted phases.

A first-order transition between the phases takes place if their energies are equal. We then obtain from (3) the dependence of the temperature of the transition between the canted and collinear phases:

$$\pm \frac{T - T_c}{T_c} = \frac{2}{3} \frac{\chi_\perp - \chi_\parallel}{\chi_\parallel} \frac{H}{\lambda M_{Fe}} + \frac{3\Delta\varepsilon}{2\chi_\parallel \lambda M_{Fe} H} \tag{4}$$

(the minus and plus signs are for the low- and high–temperature transitions). Here $\Delta\varepsilon = \varepsilon_{col} - \varepsilon_{can}$ is the difference between the anisotropy energies of the collinear and canted phases. An equilibrium transition of first order between phases of one type should take place at $T = T_c$, just as in an ideal crystal.

Equation (4) describe well (solid lines in Fig. 5) the experimental results. When account is taken of the experimentally obtained values, namely: the values of T_c corresponding to temperatures at which the dashed lines on Fig. 5 converge; the slopes of the phase-transition lines $|dH/dT|$ at $H \gtrsim 5$ kOe; the temperature width $2\Delta T$ of the "throat" of the phase diagram (curves 1–3 on Figs. 4 and 5a, and the values of the field H at which the low- and high-temperature phase transitions take place at the same temperature (curve 4 on Fig. 4 and 5b). (The theoretical curves were left out of Fig. 4 for simplicity.)

CALCULATION OF THE SHAPE OF THE BOUNDARY BETWEEN THE COLLINEAR AND CANTED PHASES NEAR A DISLOCATION

Relation (4) explains now the behavior of the boundary of the collinear and canted phases: When the temperature or field changes, the boundary traces a sequence of profiles of equal energy $\Delta\varepsilon$. Near the dislocation we have

$$\Delta\varepsilon = \Delta\varepsilon_0 - \Lambda_{ijmn}\sigma_{ij}(\alpha_m^{col}\alpha_n^{col} - \alpha_m^{can}\alpha_n^{can}), \tag{5}$$

where $\sigma_{ij} = G\tilde{b}\Phi_{ij}(\varphi)/2\pi\rho(1 - \nu)$ are the components of the

tensor of the dislocation microstresses $(i, j = x, y, z;$ the z axis is parallel to the dislocation axis), expressed in cylindrical coordinates (ρ, φ); G is the shear modulus, ν is the Poisson coefficient; $\Phi_{ij}(\varphi)$ are dimensionless functions of the angle φ and depend on the orientation and type of the dislocation; $\tilde{b} = b_1$ is the edge component of the Burgers vector $\mathbf{b}$ of the dislocation at $ij = xx, yy, xy, zz$ or $\tilde{b} = b_2(1 - \nu)$ at $ij = xz$, yz (b_2 is the screw component of the Burgers vector); Λ_{ijmn} are the components of the magnetostriction tensor and can be expressed in terms of the magnetostriction coefficients Λ_{111} and Λ_{100} that correspond to magnetization of the crystal along the $\langle 111 \rangle$ and $\langle 100 \rangle$ axis; α_m^{col} and α_m^{can} are the direction cosines of the magnetization of the collinear and canted phases, respectively.

The difference $\Delta\varepsilon_0$ between the energies of the collinear and canted phases, induced in the course of the growth or produced by stresses from other sources, will be assumed in first-order approximation to be constant in the considered region near the dislocation. The boundary between the collinear and canted phases will then describe a contour with $\Delta\varepsilon = $ const:

$$\rho = d\Phi(\varphi), \tag{6}$$

where the characteristic dimension is

$$d = \Lambda_{111} Gb [2\pi(1 - \nu)(\Delta\varepsilon_0 - \Delta\varepsilon)]^{-1} \tag{7}$$

and the dimensionless function of the angle φ is

$$\Phi(\varphi) = \frac{\Lambda_{ijmn}}{\Lambda_{111}} \frac{\tilde{b}}{b} \Phi_{ij}(\varphi)[\alpha_m^\kappa \alpha_n^\kappa - \alpha_m^\gamma \alpha_n^\gamma]. \tag{8}$$

Given T and H, the transition takes place at the point $\rho(\varphi)$, where $\Delta\varepsilon$ takes on the value determined from (3). If $\Delta\varepsilon > \Delta\varepsilon_0$, a rosette of the canted phase appears around the dislocation. As $\Delta\varepsilon \to \Delta_0$ its dimension increases [see (7)], and at $\Delta\varepsilon < \Delta\varepsilon_0$ the canted phase already occupies the main volume around the dislocation, while the collinear phase compresses into a rosette which is symmetrical to the previously considered canted-phase rosette relative to the dislocation axis.

The dislocation around which formation of the magnetic rosettes shown in Fig. 1 was observed has a glide plane $(11\bar{1})$. The minimum Burgers vector of such a dislocation is $b = a[011]$ (a is the lattice constant of $Gd_3Fe_5O_{12}$). The function $\Phi(\varphi)$ corresponding to it was calculated in the elastic-isotropic approximation for the experimentally investigated transition between the collinear phase with magnetization along $[11\bar{1}]$ and a canted phase with sublattices having a magnetization close to $[1\bar{1}1]$. The calculation was carried out, as in Ref. 19, using the representation of the tensors in the six-dimensional formalism. The magnetostriction coefficients used were those at $T = 296$ K; $\Lambda_{100} = 0.17 \times 10^{-6}$, $\Lambda_{111} = -2.93 \times 10^{-6}$ (Ref. 20) and $G = 7.6 \times 10^{11}$ erg/cm³, $\nu = 0.28$, and $b = a\sqrt{2} = 1.76 \times 10^{-7}$ cm. The shape of the obtained theoretical rosette (Fig. 6) agrees well enough with the experimentally observed one (see Fig. 1d). For the [111] direction, along which the lobe of the magnetic rosette has the maximum size, we have $\Phi(\varphi_{111}) = 1.01$ ($R = 1.01d$).

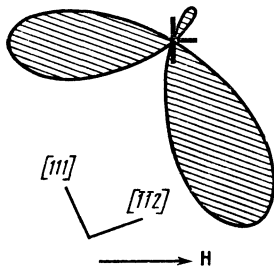From (4) and (6) we obtain an expression for the slope of the linear dependence of the temperature of the transition

FIG. 6. Theoretically calculated shape of rosette produced on a dislocation with a Burgers vector $b = a[011]$ and a glide plane $(1\bar{1}\bar{1})$ in a transition between phases with sublattice magnetizations close to the easy axes $[11\bar{1}]$ (shaded region) and $[1\bar{1}1]$.

between the collinear and canted phases on R^{-1}:

$$\frac{dT}{dR^{-1}} = \pm \frac{3\Phi(\varphi_{111})\Lambda_{111}GbT_\kappa}{4\pi(1-\nu)\chi_{\|}\lambda M_{\text{Fe}}H}. \qquad (9)$$

To conclude this section we note that, using the method proposed above, we can calculate the shape of the interphase boundary and the phase diagram in the case of any known distribution of the internal stresses in the crystal.

DISCUSSION OF RESULTS

The theoretically obtained expressions (4), (6), and (9) make it possible to estimate, on the basis of the experimental data, certain physical parameters of gadolinium iron garnets and to compare them with the values calculated in the molecular field approximation. In particular, the value $|dt/dR^{-1}| = 1.54 \times 10^{-3}$ cm deg, measured at $H = 170$ Oe, enables us to calculate from formula (9) the longitudinal susceptibility of the system $\lambda\chi_{\|} = 1.03$.

In first-order approximation, within the framework of the molecular-field theory, the magnetization M_{Gd} of the gadolinium sublattice is describerd by Eq. (1), in which the magnetic moment μ_{Gd} of the Gd^{3+} ion is equal to 7 Bohr magnetons, and $M^0_{\text{Gd}} = 124.4$ cgs emu/g. At $T = T_c = 282.5$ K we have $M_{\text{Gd}} = M_{\text{Fe}} = 22.2$ cgs emu/g (Ref. 13). If we take into account in a weak external field near T_c only the change of the magnetizations of the gadolinium sublattice $\chi_{\|} = \partial M_{\text{Gd}}/\partial H (M_{\text{Fe}} = \text{const})$ then

$$\lambda\chi_{\|} = xB_{7/2}^{-1}(x)\,dB_{7/2}(x)/dx = 0.967,$$

where $x = 0.423$ was calculated form $B_{7/2}(x) = M_{\text{Gd}}/M^M_{\text{Gd}}$ at $T = T_c$. A more accurate values $\lambda\chi_{\|} = 1.01$ is obtained by differentiating with respect to H the equations for the magnetizations of all three sublattices of the magnet $[\lambda_{11} = -61\,000, \lambda_{12} = -91\,060, \lambda_{13} = -900, \lambda_{22} = -29\,000, \lambda_{23} = -4075$ Oe-g/cgs emu, $M^0_1 = 59.3$, and $M^0_2 = 88.9$ cgs emu/g (Ref. 13)]. The theoretical and experimental values of $\lambda\chi_{\|}$ are in good agreement.

The slopes of the $H - T$ lines of the phase transition between the canted and collinear phases as 5 kOe $< H < 20$ kOe (Fig. 5) are characterized by the value $|dH/dT| \approx 12.8$ kOe/deg. Assuming that in this field interval the elastic stresses influence little the slope of the phase-transition lines (cf. Figs. 5 and 5b), we obtain from (4) $|dH/dT| = (3/2)(\chi_\perp - \chi_\|)^{-1}\chi_\|\lambda M_{\text{Fe}}T_c^{-1}$.

Here $\lambda M_{\text{Fe}}T_c^{-1} = xk/\mu_{\text{Gd}} = 900$ Oe/deg at $T = T_c$. Then, using the experimental value of $|dH/dT|$, we obtain $(\chi_\perp - \chi_\|)/\chi_\| \approx 0.11$. This quantity can be easily obtained theoretically by recognizing that the transverse susceptibility $\chi_\perp$ of a gadolinium iron garnet principally by the kink and the direction of the external field of the magnetizations of its sublattices. When account is taken of the rotation of the magnetization vectors of the gadolinium and of the two iron sublattices we have

$$\lambda\chi_\perp = 1 + \frac{M_1 + M_2}{M_1 - M_2}\cdot\frac{\lambda_{13} - \lambda_{23}}{2\lambda_{12}} \approx 1.10. \qquad (10)$$

Using $\lambda\chi_{\|} = 1.01$, we obtain $(\chi_\perp - \chi_\|)/\chi_\| \approx 0.09$. The discrepancy between the experimental and theoretical values must be regarded as very small, since the value $(\chi_\perp - \chi_\|)/\chi_\|$ is determined by the difference between close quantities $\chi_\perp$ and $\chi_\|$, which in turn are calculated on the basis of λ_{ij} measured with definite errors.

The general picture of the spin-flip phase transitions in gadolinium iron garnet, as can be seen from the foregoing estimate, is well described on the basis of the model considered by us. The good agreement obtained between the calculated curves [expressions (4) and (6)] and the experimental data (Figs. 1 and 5) is evidence that the equilibrium location of the interphase boundary in the crystals corresponds to a great degree to magnetoelastic nonequivalence of the collinear and canted phases, and that the influence of the internal stresses on the spin-flip phase transition manifests itself principally on account of the change of the magnetic anisotropy of the crystal.

The shift of the compensation temperature on account of the dilatation component of the stresses can be regarded as a less important factor, inasmuch as a noticeable change of T_c calls for higher voltages than are usually realized in the crystal. Thus, to shift T_c by 0.1 K the stresses needed are of the order of 2 kgf/mm^2 (Ref. 6), which are reached near the dislocation core only at a distance not farther than ~ 2 μm from it. Therefore the experimentally observed stronger changes of the compensation temperature over the sample (cf. Figs. 5a and b) can be connected with the concentration inhomogeneity of the composition or impurity. In this case, as seen from Fig. 5, a change of T_c leads to a temperature shift of the phase diagram as a whole.

The good agreement, not only qualitative but also quantitative, between the experimental and theoretical data uncovers prospects for the use of the determined relations for the spin-flip phase transitions for the purpose of studying the defect structure of rare-earth iron garnets. In particular, investigations of the magnetic rosette produced near the dislocation make it possible to determine the direction and magnitude of its Burgers vector.

From the distribution of the striction-nonequivalent magnetic phases in the crystal one can determine more reliably the induced anisotropy and the weaker internal stresses than by the photoelasticity method. Thus, by measuring the transition-temperature shift due to the stresses accurate, e.g., to ± 0.1 K we can record a stress level of the order of 2 kgf/cm^2.

Finally, measurements of the temperature shift of the

phase transitions as a function of the level of the microscopic (residual or induced) stresses or near a dislocation with known characteristics, can also be used to determine the microscopic parameters of an iron garnet with a compensation point.

[1] V. L. Ginzburg, Usp. Fiz. Nauk 134, 469 (1981) [Sov. Phys. Usp. 24, 585 (1981)].
[2] A. E. Borovik and I. N. Nechiporenko, Fiz. Nizk. Temp. 4, 218 (1978) [Sov. J. Low Temp. Phys. 4, 108 (1978)].
[3] I. M. Dubrovskiĭ and M. A. Krivoglaz, Zh. Eksp. Teor. Fiz. 77, 1017 (1979) [Sov. Phys. JETP 50, 512 (1979)].
[4] A. P. Levanyuk, V. V. Osipov, A. S. Sigov, and A. A. Sobyanin, ibid. 76, 345 (1979) [49, 176 (1979)].
[5] K. P. Belov, A. K. Zvezdin, A. M. Kadomtseva, and R. Z. Levitin, Orientatsionnye prekhody v redkozemel'nykh magnetikakh (Orientational Transitions in Rare-Earth Magnets), Nauka, 1979.
[6] N. F. Kharchenko, V. V. Eremenko, and S. L. Gnatchenko, Zh. Eksp. Teor. Fiz. 69, 1697 (1975) [Sov. Phys. JETP 42, 862 (1975)].
[7] S. L. Gnatchenko and N. F. Kharchenko, ibid. 70, 1379 (1976) [43, 719 (1976)].
[8] N. F. Kharchenko, V. V. Eremenko, S. L. Gnatchenko, L. I. Belyĭ, and E. M. Kabanova, ibid. 68, 1073 (1975) [41, 531 (1975)].
[9] K. P. Belov, L. A. Chernikova, E. V. Talalaeva, R. Z. Levitin, T. V. Kudryavtseva, S. Amadezi, and V. N. Ivanovskiĭ, Zh. Eksp. Teor. Fiz. 58, 1923 (1970) [Sov. Phys. JETP 31, 1035 (1970)].
[10] R. Z. Levitin, B. K. Ponomarev, and Yu. F. Popov, ibid. 59, 1952 (1970) [32, 1056 (1971)].
[11] E. L. Smirnova, V. I. Smirnov, and Yu. I. Ukhanov, Izv. AN SSSR ser. fiz. 25, 1186 (1971); Pis'ma Zh. Eksp. Teor. Fiz. 11, 435 01970) [JETP Lett. 11, 293 (970)].
[12] J. L. Feron, G. Fillon, and F. Hug, J. de Phys. 34, 247 (1973).
[13] J. Bernssconi and D. Kuse, Phys. Rev. B3, 811 (1971).
[14] O. A. Grzhegorzhevskiĭ and R. V. Pisarev, Zh. Eksp. Teor. Fiz. 65, 633 (1973) [Sov. Phys. JETP 38, 312 (1974)].
[15] V. K. Vlasko-Vlasov, L. M. Dedukh, and V. I. Nikitenko, Fiz. Tverd. Tela (Leningrad) 23, 1857 (1981) [Sov. Phys. Solid State 23, 1085 (1981)].
[16] V. I. Nikitenko and L. M. Dedukh, Phys. Stat. Sol. (a) 3, 383 (1970).
[17] J.-F. Krumme and P. Hansen, Appl. Phys. Lett. 22, 312 (1973).
[18] A. F. Popkov, Fiz. Tverd. Tela (Leningrad) 18, 357 (1976) [Sov. Phys. Solid State 18, 209 (1976)].
[19] L. M. Dedukh, M. V. Indenbom, and V. I. Nikitenko, Zh. Eksp. Teor. Fiz. 80, 380 (1981) [Sov. Phys. JETP 53, 194 (1981)].
[20] A. E. Clark, J. J. Rhyne, and E. R. Callen, J. Appl. Phys. 39, 573 (1968).

Translated by J. G. Adashko